Silver Nanoparticle Detection in Real World Environments via Particle Impact Electrochemistry

Xiuting Li[‡], *Christopher Batchelor-McAuley, Richard G. Compton*[*]

Department of Chemistry, Physical and Theoretical Chemistry Laboratory, University of Oxford, South Parks Road, Oxford OX1 3QZ, UK

Corresponding Author

*Correspondence to: richard.compton@chem.ox.ac.uk

Telephone number: +44)0(1865 275957

Keywords

Agglomeration, Capping Agent, Single Particle Analysis, UV-vis, Real-world media

Abstract

Silver nanoparticles (AgNPs) suspended in bottled mineral water and in tap water were successfully detected via the nano-impact method without the deliberate addition of electrolyte. The recorded spike charge was used to indicate the stability of the AgNPs in their suspensions. It is found that the AgNPs largely agglomerated in potable water within the first 20 minutes. Addition of high concentrations of citrate (>2mM) improved the stability of the AgNPs and enabled the detection and sizing of the AgNPs monomers in these media. Aging of the potable water suspensions was independently confirmed via UV-vis spectroscopy, validating the electrochemical method for detecting nanoparticles in real world media.

The optical, electronic, catalytic, mechanical properties of nanoparticles in comparison with the corresponding bulk materials have triggered enormous worldwide activity in the synthesis of manmade nanoparticles for a myriad of applications. The rapid growth in the use of manmade nanoparticles necessarily raises concerns relating to the extent to which such materials enter the environment and their consequent impact. Studies have suggested the possibility of significant nano-toxicity effects although these are notoriously difficult to prove.[1-2] A key limitation to nano-toxicity studies is the requirement for rapid, relatively cheap, reliable and versatile methods for the analysis of nanoparticles especially in the solution phase. Such analysis needs to embrace chemical composition, size, concentration and state of aggregation/agglomeration but such information severely challenges existing techniques. Transmission electron microscopy (TEM) and scanning electron microscopy (SEM) are generally ex-situ methods. Although the use of liquid cell[3] TEM based techniques are becoming more prevalent, first beam damage remains a serious issue[4-5] and second the thickness of the cells are necessarily limited to maximally a few hundred nanometers and even at these scales the solution thickness significantly limits the spatial resolution of the system.[6] Moreover, if nanoparticle volume distributions and hence nanoparticle concentrations are desired then either more advanced TEM imaging techniques such as tomography[7-8] need to be employed or alternately the 2D imaging needs to be coupled with a complementary technique such as AFM[9] to provide a measure of particle heights. Light scattering techniques enable nanoparticles to be studied under conditions that more authentically reflect the real world environment; however, these methodologies too are not without their limitations, for example, Dynamic Light Scattering (DLS) are commonly limited to relatively monodisperse samples[10-11] and nanoparticle tracking analysis (NTA) fails for particles smaller than ca 25nm.[8] Moreover, for plasmonic nanoparticles such as those fabricated from silver and gold, the agglomeration level of the material may be monitored

optically by studying the shift in the adsorption wave, providing a sensing platform for the detection of metal ions.[12-13]

As one of the most commonly used nanoparticles, a considerable quantity of nano-silver has been accumulated in water, soil, plants and animals in the food chain.[14-16] The nano-toxicity of these materials has been suggested to potentially arise from the generation of hydrogen peroxide from oxygen via the oxidative dissolution of the particles.[17-18]

An easy, cost-effective and reliable method for in-situ analysis of silver nanoparticles in real world media especially in the solution phase is very desirable. The particle-electrode collision (so-called nano-impacts) is one of the emerging popular methods for the in-situ detection of nanoparticles.[19-24] As one of various processes involved in the nano-impact method, the so-called 'direct' impacts are of paramount significance and involve the electrolysis of the nanoparticle itself.[25] For example single silver nanoparticles in solution impact a microelectrode held at a suitable electrical potential and become oxidised to soluble silver (Ag^+) cations or to AgCl.[26] The impact is signalled by a current spike at the electrode. The charge (Coulombs) obtained by integrating the current transients reflects (via Faraday's 1st Law) the number of atoms (or molecules) in the nanoparticle thus giving its size. Note that silver nanoparticles are typically at least quasi-spherical if not more irregular in shape so numbers of atoms may be a better measure of size than a radius.[8]

A large number of current spikes are easily and rapidly measured so giving a particle size distribution. The change in the spike charge can also be used to reflect the aging processes of the nanoparticles in their suspensions such as might arise from agglomeration and/or aggregation. In this work, we develop a simple and reliable electrochemical methodology based on the 'direct' nano-impact technique, for in-situ characterization of AgNPs in potable water media. Both bottled mineral water and kitchen tap water were investigated and AgNPs

are found to agglomerate in these media according to the increased spike charge compared with the expected charge for a single AgNP. Citrate was used to improve the stability of AgNPs so that the sizing of the AgNP monomer particles from the spike charge was realised for comparison.

Experimental section

Chemicals

Quasi-spherical '20 nm diameter' citrate capped-AgNPs were synthesised using a seeded growth method as 0.13 mg/mL containing 2 mM of sodium citrate.[27-28] Potassium chloride (≥99.5%) and tri-sodium citrate (99.0%) were purchased from Sigma-Aldrich and British Drug Houses respectively. Both of them were used as received without further purification. *Evian* bottled mineral water was brought from local supermarket (content of mineral ions is shown in SI section 4) and tap water was directly obtained from the Rodney Porter Building, University of Oxford. Except the indicated potable water samples, all the other solutions were prepared with deionized water (Millipore) with a resistivity of 18.2 MΩ.cm at 298 K.

TEM Sizing of the AgNPs

Transmission electron microscopy (TEM, 300 kV JEOL 3000F microscope) was used to determine the size of the AgNPs. Samples were prepared by dropcasting the AgNPs suspension (0.013 mg/mL silver, 0.2 mM sodium citrate) onto carbon grids (Agar Scientific, Stansted, U.K.), followed by drying in air prior to imaging. The resulting nanoparticles images were sized using Image J software (National Institutes of Health, U.S), giving the size of the synthesised AgNPs as 20.1 ± 4.3 nm.

Stability of the AgNPs in different media

The stabilities of AgNPs in 20 mM KCl, bottled mineral water, kitchen tap water, bottled mineral water containing 2 mM citrate and kitchen tap water containing 2 mM citrate were studied via UV/Vis measurements (l = 300-800 nm) with a Shimadzu UV-1800 spectrophotometer in disposable cuvettes (Eppendorf UVette, Sigma-Aldrich) using a 10 mm optical path length. UV/Vis spectra were recorded over a 60 min period after the AgNPs stock solution (48 pM) was separately added to form suspensions of 12 pM AgNPs in each media.

Nano-impact experiments

The electrochemistry setup was equipped with a homemade thermostat system which was fabricated using a Peltier-effect heat pump.[29] The temperature of the solution was controlled at 25.0 ± 0.1 °C by a temperature probe (PT100 Sensor, R. S. Components Ltd, Corby, UK) immersed in the solution. Nano-impact experiments were carried out using the homemade thermostat system with a home-built low noise potentiostat which was described previously.[30] For the latter, a low-noise current amplifier (LCA-4K-1G, FEMTO Messtechnik GmbH, Germany) was used. The signal was digitised at 100 KS/s via a USB data acquisition device (USB-6003, National Instruments, Texas, US) and subsequently filtered digitally by a 4-pole Bessel filter to 100 Hz using a script written in Python. Bessel filters have been demonstrated to conserve the total charge transferred in an impact event.[31]

Measurements were conducted with a three-electrode system in a Faraday cage. A carbon microdisc electrode of normally 33μm diameter (IJ Cambria Scientific Ltd, UK) was used as the working electrode. Note that this commercially supplied electrode exhibited a radius of 21.4 μm on calibration with ferrocenemethanol solution (Figure S1) using a diffusion coefficient reported by Mirkin at 25 °C.[32] A leakless Ag/AgCl (3.4 M KCl, eDAQ) and a platinum foil (Goodfellow, Cambridge, U.K.) acted as the reference electrode and the

counter electrode respectively. The working electrode was polished with alumina powders from Buehler, Lake Bluff, IL, U.S.A., of decreasing sizes: 1.0, 0.3, and 0.05µm, followed by a thorough rinse with deionized water and drying under a Nitrogen atmosphere. Chronoamperometry was performed separately on 20 mM KCl, bottled mineral water and kitchen tap water containing 12 pM AgNPs but no deliberately added electrolyte except where specified and using the carbon microdisc working electrode. The potential was held at 0.8 V (vs. leakless Ag/AgCl) for 60 s. A chronoamperogram was recorded in the each suspension after aging for different time ranging from 0-70min. Comparative experiments were conducted in the bottled mineral water and kitchen tap water suspensions containing 2mM citrate. Note that the citrate ions were introduced into these media before the AgNPs stock suspension were added- the order in which electrolyte components are added can influence the nanoparticle sol stability. Nano-impact spikes were identified and analysed using a script written in Python 3.5.[33]

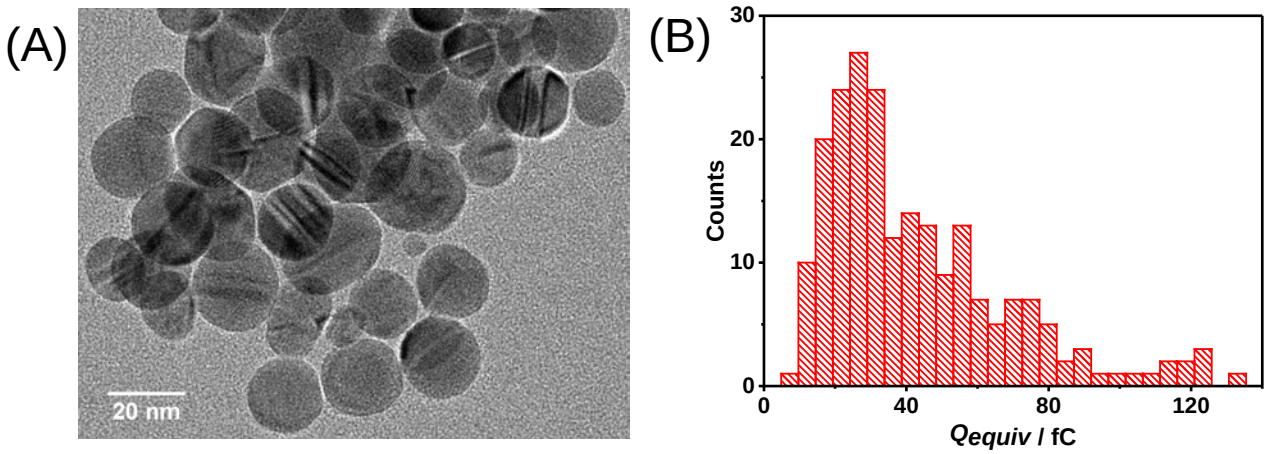

Figure 1. (A) A representative TEM image of the AgNPs; (B) Histogram showing the equivalent charge distribution each values derived from the TEM sizing.

Results and discussion

First the AgNPs were characterised by Transmission Electron Microscopy (TEM) to allow the expected charge distribution for the oxidation of the AgNPs to be predicted via Faraday's first law. Second, we performed the nano-impacts of AgNPs in 20mM KCl, bottled mineral water and kitchen tap water respectively. AgNPs in the potable water samples were detected as current spikes on recorded chronoamperograms. The charge passed per event was more than the expected value from the TEM analysis, indicating the likely agglomeration of the AgNPs.[34] Third, citrate was deliberately introduced into the water samples prior to analysis to improve the stability of the AgNPs for the purpose of detecting and sizing AgNP monomers from their corresponding spike charge. Finally, the stability of the AgNPs in these media was further investigated with UV-vis spectroscopy.

The consistency between the results from UV-via analysis and the nano-impact further validates the nano-impact for the detection, sizing and agglomeration state determination of the AgNPs in real world environments.

Transmission electron microscopy (TEM) was first used to characterise the in-house synthesised AgNPs. A representative TEM image is shown in Figure 1(A). It can be observed that most of the nanoparticles have a quasi-spherical shape. A small percentage of the sample shows certain levels of *significant* non-sphericity, which is likely due to the presence of various facets.[35] This non-spherical nature of the particles creates a challenge to determining the nanoparticle number concentration; more accurate nanoparticle volume estimates can be achieved through the use of tomography based imaging techniques.[8] However, in the present work the size analysis of the nanoparticle is provided on the basis of a series of 2D images and in accordance with previous work the 'average' particle diameter, as measured on the basis of the particles projected area, has been used to quantify the size of the particles.[8] 220

nanoparticles were analysed in total, giving an average diameter of 20.1 ± 0.3 nm (the error of the mean charge is the standard error of the mean given by $SD/n^{1/2}$ where SD is the standard deviation and n is the number of spikes). The size of the AgNPs as measured was then converted via Faraday's first law and presented in terms of an equivalent total charge (Q_{equiv}), as shown in Figure 1(B). The average Q_{equiv} is 40.5 ± 1.8 fC which compared below with the experimental charge transferred per event in the nano- impact measurements. Note that the inference of the charge from the two-dimensional TEM images may cause certain level of error especially for those NPs with significantly non-spherical shapes.

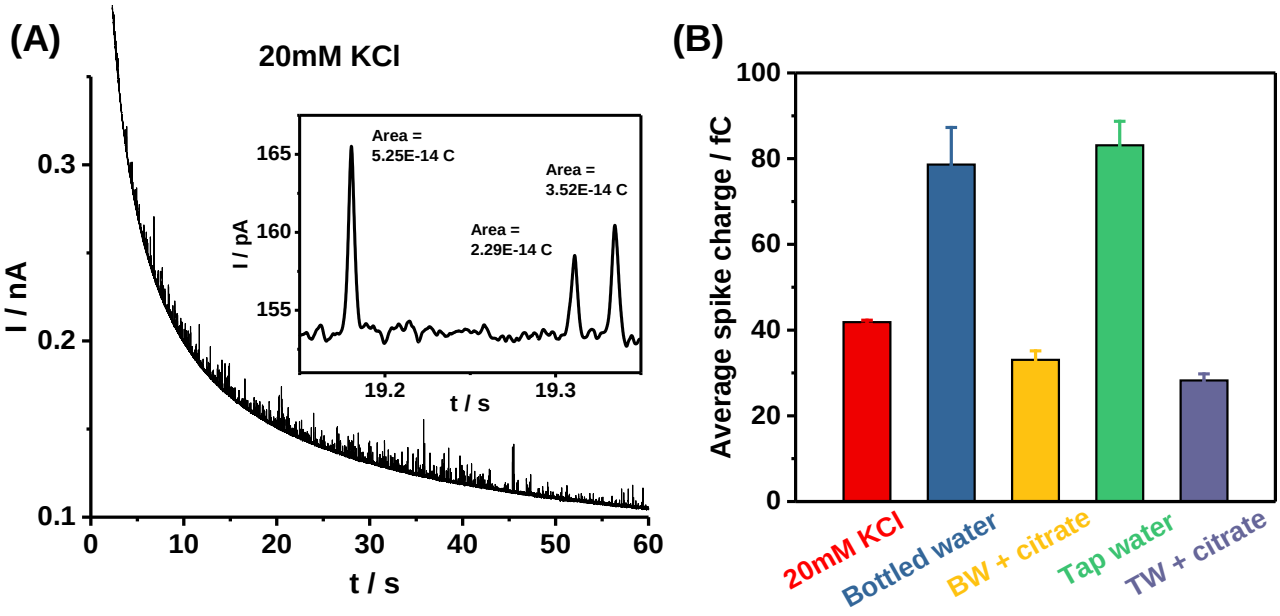

Figure 2. (A) Representative chronoamperometric profiles of 12pM AgNPs aged for around 20 min in 20 mM KCl (A) at 0.8V vs Ag/AgCl (3.4 M KCl) at a carbon microdisc electrode (r = 21.4 μm); (B) The bar graph shows the spike charge in 20 mM KCl, bottled mineral water, kitchen tap water, bottled mineral water containing 2 mM citrate and kitchen tap water containing 2 mM citrate.

Nano-impact experiments were then performed to study the electrochemical responses of AgNPs oxidation in-situ in 20 mM KCl and the potable water samples. AgNPs in their suspension diffuse randomly by virtue of Brownian motion. Once an AgNP hits the electrode

held at a suitable potential, it is oxidized resulting in a current-transient spike in chronoamperometry. Figure 2(A) shows a representative chronoamperomograms measured at a carbon microdisc electrode (r = 21.4 μm) immersed in 12pM AgNP suspensions which were aged for 20 min in 20mM KCl at 0.8V vs Ag/AgCl (3.4M KCl). The inlays clarify the representative spike shapes and their corresponding charge values. This concentration of AgNPs was chosen based on the optimised spike frequency for which both the resolution of the recorded spikes and measurement efficiency were considered. In 20mM KCl, spikes were observed at a frequency of 5.8 ± 1.2 s^{-1} (which compares to the diffusion-limited expected frequency: 15.0 s^{-1}, note this diffusion limited value represents an upper limit and does not account for hindered diffusion[36] or the influence of electrode shielding[22]) with an average charge transferred per spike of 36.0 ± 0.5 fC. It has been reported that the low experimental spike frequency is not necessarily related to nanoparticle mass transport, but possibly reflects that not every AgNPs arriving at the electrode surface is oxidised.[37] Each spike charge was treated with diffusional weighting (SI section 2), giving the average value of 41.8 ± 0.5 fC. This is very close to the expected charge (40.5 fC) for a spherical AgNP with a radius of 10.1 nm according to the TEM images (Figure 1), indicating the fully oxidation of AgNPs in the impacting events.

Figure S2 presents the corresponding chronoamperograms of 12pM AgNP aged for 20 min in bottled mineral water (A) and in kitchen tap water (B) respectively. It can be observed that for the AgNPs in the bottled water and tap water the frequency of spikes is significantly lower (0.2 s^{-1} in bottled water and 0.6 s^{-1} in tap water) than that in 20mM KCl. This low frequency is likely due to the lower chloride ions concentrations in the potable water samples; work reported in the literature has previously noted that the nano-impact frequency is under some conditions sensitive to a solution halide concentration.[38] This halide sensitivity has been previously understood in terms of the sluggish nucleation kinetics associated with AgCl

formation.[37] The average spike charge after diffusional weighting is 78.6 ± 8.7 and 83.1 ± 5.6 fC for bottled water and tap water suspensions respectively, around twice of the charge value (41.8 ± 0.5 fC) obtained in 20mM KCl, indicating that the AgNPs partially agglomerate in the bottled water and tap water. This is likely attributed to the presence of trace amounts of multivalent ions in the potable water samples (SI section 4) which significantly screens the negative surface charge of the citrate-caped AgNPs even though its ion strength is lower than that in 20mM KCl.[39-40] The longer term (i.e. days) stability of the nanoparticle suspension is a more complex issue, due to the presence of oxygen a significant fraction of the material can be transformed. These oxidation kinetics in real-world potable water samples - in contrast to the case in which nanoparticle dissolution is studied in de-ionised water[18] – are variable and can be highly sensitive to the presence of trace ions. That said the above demonstrates that by using the nanoimpact method AgNPs in potable water samples can be detected and their agglomeration demonstrated.

Having evidenced the formation of AgNP agglomerates in bottled water and tap water, citrate was then deliberately added to inhibit the agglomeration of AgNPs for the purpose of sizing the AgNP monomers. As shown in Figure S2(C) and (D), in the presence of 2mM citrate, the spike frequency of the bottled water (0.2 s^{-1}) and tap water (0.4 s^{-1}) suspensions is also much lower than that of 20mM KCl because of the slow initiation of the AgCl nucleation in these media containing low concentrations of chloride. However, in the presence of 2mM citrate, the average spike charge after diffusional weighting becomes 33.1 ± 2.1 and 29.8 ± 1.8 fC for the bottled water and tap water, giving the mean effective radius of the AgNPs of 9.2 ± 0.2 and 8.8 ± 0.1 nm respectively. This charge for the individual particles as experimentally measured in the presence of higher citrate concentrations is less than expected on the basis of the above TEM analysis. Either this indicates that a) the nanoparticle volume has been 'overestimated' in the TEM analysis[8] or b) the presence of the citrate causes a size sensitivity

leading to the probability of experimentally observing larger particles being partially being reduced. As can be seen in SI section 3 the presence of the citrate reduces the observed nano-impact frequency and furthermore nano-impact experiments are known to be sensitive to the presence of organics.[41] However, the bar graph in Figure 2(B) depicts the average spike charge of the AgNPs in 20mM KCl, bottled mineral water, kitchen tap water, bottled mineral water containing 2mM citrate and kitchen tap water containing 2mM citrate. It clearly indicates that the initial agglomeration of the AgNPs occurred in these potable water samples without citrate and was effectively inhibited in the presence of 2mM citrate. In the latter case, the AgNPs monomers were therefore able to be sized from the recorded spike charge values. This inhibition of the nanoparticle agglomeration is further evidenced optically, *vide infra*.

Since the ability of the nano-impact technique to detect AgNPs in different media has been demonstrated, the stability of the AgNPs in these media over a relatively long period was further investigated electrochemically. The charge transfer for each spike is indicative of agglomeration state[42] of the impacting AgNPs, and therefore can be used to evidence the detailed agglomeration process of the AgNPs. Chronoamperograms with duration of 60 s were recorded after different aging time for the AgNPs in 20mM KCl, bottled mineral water, kitchen tap water, bottled mineral water containing 2mM citrate and kitchen tap water containing 2mM citrate respectively at 0.8V vs Ag/AgCl (3.4M KCl). Figure 3(A) shows the average spike charge on each chronoamperogram recorded in 20mM KCl (red curve), bottled mineral water in the absence (blue curve) and presence (yellow curve) of 2 mM citrate over a period of 70 min. It can be seen that the average spike charge obtained in 20mM KCl is relatively stable at around 35 fC over 70 min, indicating the good stability of the AgNPs during the whole period of the measurements. While the average impact charge of the AgNPs in bottled water exhibits an obvious increase from around 35 fC to 70 fC within the first 20 min of measurement and presents nearly a plateau after 20 to 70 min. This suggests that the

agglomeration process of the AgNPs in bottled water mainly occurs at the first 20 min; possibly as an equilibrium population of monomers, dimers, trimers etc. is formed.[43] When 2mM citrate was added to the bottled water prior to introducing the AgNPs stock solution, the spike charge remained at ca. 35 fC over the whole period demonstrating the improved stability of AgNPs in bottled water in the presence of citrate. Analogous experiments were also conducted with the tap water suspension and very similar phenomena were observed, as shown in Figure 3B. In addition, the spikes collected during 20 to 70 min of aging were further analysed and the relative cumulative frequency charge distribution was shown in Figure 3(C) and (D). Again, the agglomeration of the nanoparticles in bottled water and tap water was clearly indicated and the inhibition of citrate on the agglomeration was demonstrated.

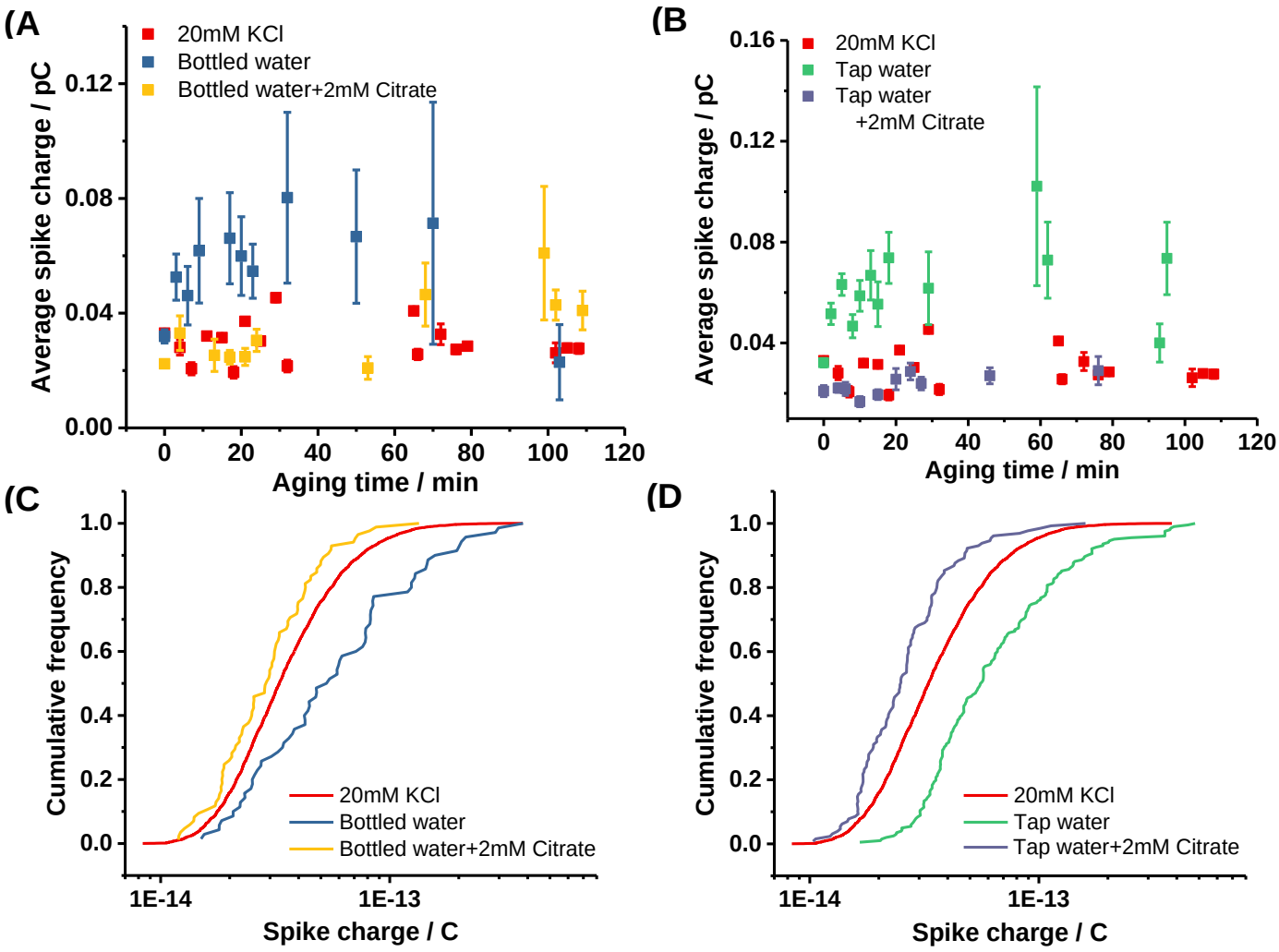

Figure 3. Plots of the average spike charge vs aging time of 12pM AgNPs in 20mM KCl, bottled water (A) and tap water (B) in the absence and presence of 2mM citrate up to a two hour time period; (C) and (D) showing the corresponding cumulative frequency charge distributions for nano-impact spikes collected during 20 to 70 min of aging with applying a diffusional weighting.

The stability of AgNPs in the above media was further investigated by means of UV–Vis spectroscopy. AgNPs display plasmonic responses[44] where the position and the magnitude of the peak are related to size, shape, concentration and environment of the particles respectively.[45] The magnitude of the peak absorbance is more sensitive to the change in the nanoparticle suspension and therefore was mainly used to assess their stabilities. Figure S2

shows the UV–Vis spectra for the suspensions of 12pM AgNPs in 20mM KCl, bottled mineral water, bottled mineral water containing 2mM citrate, kitchen tap water and kitchen tap water containing 2mM citrate over a 60 min period at a 2 min interval in the first 10 min and 10 min interval for the rest. The corresponding UV–Vis spectra for the AgNPs suspensions aged for 20 min in the above media are presented in Figure 4(A). It can be seen that absorbance peak of all suspensions occurs near 390 nm. Figure 4B depicts the peak absorbance against the aging time in all cases over the 60 min period. The magnitude of the peak in 20mM KCl is relatively stable and drops by only 3% after 20 min and 10% after 60 min. This loss is possibly due to the oxidative dissolution of the nanoparticles in the presence of the small amount of dissolved oxygen.[18] In contrast the peak absorbance in the suspensions of bottled water and tap water shows significant decreases of 68% and 67% respectively after 20 min, 71% and 74% after 60 min. In addition, as shown in Figure 3A, after 20 min of aging a board peak at around 600 nm arises for the bottled water suspension (blue curve) and high absorbance plateau above the background across the high wavelength region for the tap water suspension (green curve). This is indicative of the agglomeration of the nanoparticles in these water samples.[46] The better stability of the nanoparticles in 20 mM KCl than that in the potable water samples is likely ascribed to presence of inorganic di- and tri-valent ions in the potable water sample. It is further observed that after adding 2mM citrate into the potable water suspensions, the peak absorbance after 20 min and 60min of aging remains 70% and 60% of the initial value for the bottled water suspension in comparison with 97% and 90% for the tap water suspension respectively. This indicates that the citrate greatly improves the stability of the nanoparticles in these water samples. The above observation is entirely consistent with the results from the nano-impact experiments. Both reflect the tendency of AgNPs to agglomerate in potable water and the process mainly occurs at the first 20 min after formation of the suspensions; the agglomeration can be effectively inhibited by introducing citrate.

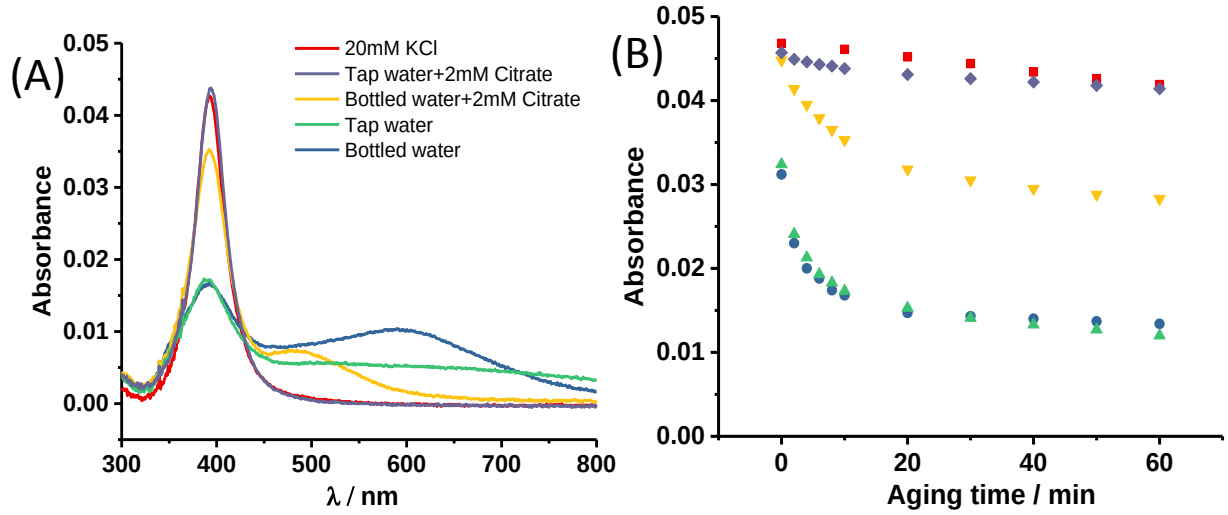

Figure 4. (A) UV-vis absorbance spectra of 12pM AgNPs aged for 20 min in 20mM KCl (red curve), bottled mineral water (blue curve), bottled mineral water containing 2mM citrate (yellow curve), kitchen tap water (green curve) and kitchen tap water containing 2mM citrate (purple curve); (B) peak absorbance with time in the above media.

Conclusions

AgNPs in potable water can be detected electrochemically via the nano-impact method. The approximately doubled spike charge of that in 20 mM KCl indicates the agglomeration of the AgNPs and the formation of primarily AgNPs dimers in the bottled water and tap water. The stability study over around one hour reflects that this agglomeration process mainly occurs in the first 20 min following formation of the nanoparticle suspension. The addition of citrate into the potable water was shown to inhibit the agglomeration and to enable the detection and sizing of AgNP monomers. Further investigation with UV-vis spectroscopy shows very good consistency with the nano-impact results, validating the ability of the latter on detection, sizing and agglomeration state determination of the AgNPs in the real world media. The present method holds potential for the characterization of various nanomaterials in real world environments.

ASSOCIATED CONTENT

Supporting Information Available: The following file is available free of charge.

SI.docx: Data relating to the calibration of the microdisc electrode; Further information on diffusional weighting of the spike charge; Silver nano-impact response in different media; Composition of the mineral water and the UV-vis spectra of the silver nanoparticles as a function of time.

AUTHOR INFORMATION

‡ Present Address: Institute for Advanced Study, Shenzhen University, Shenzhen, China

Corresponding Author

*E-mail: richard.compton@chem.ox.ac.uk. Telephone: +44(0) 1865 275957

Notes

The authors declare no competing financial interests.

ACKNOWLEDGMENT

This project has received funding from the European Research Council (ERC) under the European Union's Horizon 2020 research and innovation programme (grant agreement No. 727292) and from the European Research Council under European Union's Seventh Framework Programme)FP/207-2013(, ERC Grant Agreement no. 320403.

References

1. Valsami-Jones, E.; Lynch, I., How Safe Are Nanomaterials? *Science* **2015**, *350*, 388-389.
2. Haase, A.; Lynch, I., Quality in Nanosafety — Towards Reliable Nanomaterial Safety Assessment. *NanoImpact* **2018**, *11*, 67-68.
3. Ross, F. M., *Liquid Cell Electron Microscopy*; Cambridge University Press: Cambridge, 2017.

4. Keskin, S.; De Jonge, N., Reduced Radiation Damage in Transmission Electron Microscopy of Proteins in Graphene Liquid Cells. *Nano Lett.* **2018**, *18*, 7435-7440.
5. Liao, H.-G.; Zherebetskyy, D.; Xin, H.; Czarnik, C.; Ercius, P.; Elmlund, H.; Pan, M.; Wang, L.-W.; Zheng, H., Facet Development During Platinum Nanocube Growth. *Science* **2014**, *345*, 916-919.
6. de Jonge, N., Theory of the Spatial Resolution of (Scanning) Transmission Electron Microscopy in Liquid Water or Ice Layers. *Ultramicroscopy* **2018**, *187*, 113-125.
7. Scott, M. C.; Chen, C.-C.; Mecklenburg, M.; Zhu, C.; Xu, R.; Ercius, P.; Dahmen, U.; Regan, B. C.; Miao, J., Electron Tomography at 2.4-Ångström Resolution. *Nature* **2012**, *483*, 444.
8. Little, C. A.; Batchelor-McAuley, C.; Young, N. P.; Compton, R. G., Shape and Size of Non-Spherical Silver Nanoparticles: Implications for Calculating Nanoparticle Number Concentrations. *Nanoscale* **2018**, *10*, 15943-15947.
9. Attota, R. K.; Liu, E. C., Volume Determination of Irregularly-Shaped Quasi-Spherical Nanoparticles. *Analytical and Bioanalytical Chemistry* **2016**, *408*, 7897-7903.
10. Anderson, W.; Kozak, D.; Coleman, V. A.; Jämting, Å. K.; Trau, M., A Comparative Study of Submicron Particle Sizing Platforms: Accuracy, Precision and Resolution Analysis of Polydisperse Particle Size Distributions. *J. Colloid Interface Sci.* **2013**, *405*, 322-330.
11. Filipe, V.; Hawe, A.; Jiskoot, W., Critical Evaluation of Nanoparticle Tracking Analysis (Nta) by Nanosight for the Measurement of Nanoparticles and Protein Aggregates. *Pharmaceutical research* **2010**, *27*, 796-810.
12. Yoosaf, K.; Ipe, B. I.; Suresh, C. H.; Thomas, K. G., In Situ Synthesis of Metal Nanoparticles and Selective Naked-Eye Detection of Lead Ions from Aqueous Media. *J. Phys. Chem. C* **2007**, *111*, 12839-12847.
13. Chen, X.; Cheng, X.; Gooding, J. J., Multifunctional Modified Silver Nanoparticles as Ion and Ph Sensors in Aqueous Solution. *Analyst* **2012**, *137*, 2338-2343.
14. Gottschalk, F.; Sonderer, T.; Scholz, R. W.; Nowack, B., Modeled Environmental Concentrations of Engineered Nanomaterials (Tio2, Zno, Ag, Cnt, Fullerenes) for Different Regions. *Environmental Science & Technology* **2009**, *43*, 9216-9222.
15. Harris, A. T.; Bali, R., On the Formation and Extent of Uptake of Silver Nanoparticles by Live Plants. *Journal of Nanoparticle Research* **2008**, *10*, 691-695.
16. Lankveld, D. P. K.; Oomen, A. G.; Krystek, P.; Neigh, A.; Troost – de Jong, A.; Noorlander, C. W.; Van Eijkeren, J. C. H.; Geertsma, R. E.; De Jong, W. H., The Kinetics of the Tissue Distribution of Silver Nanoparticles of Different Sizes. *Biomaterials* **2010**, *31*, 8350-8361.
17. Batchelor-McAuley, C.; Tschulik, K.; Neumann, C. C.; Laborda, E.; Compton, R. G., Why Are Silver Nanoparticles More Toxic Than Bulk Silver? Towards Understanding the Dissolution and Toxicity of Silver Nanoparticles. *Int J Electrochem Sci* **2014**, *9*, 1132-8.
18. Liu, J.; Hurt, R. H., Ion Release Kinetics and Particle Persistence in Aqueous Nano-Silver Colloids. *Environmental science & technology* **2010**, *44*, 2169-2175.
19. Cheng, W.; Compton, R. G., Electrochemical Detection of Nanoparticles by 'Nano-Impact' Methods. *Trends Anal. Chem.* **2014**, *58*, 79-89.
20. Pumera, M., Impact Electrochemistry: Measuring Individual Nanoparticles. *ACS Nano* **2014**, *8*, 7555-7558.
21. Rees, N. V., Electrochemical Insight from Nanoparticle Collisions with Electrodes: A Mini-Review. *Electrochem. Commun.* **2014**, *43*, 83-86.
22. Sokolov, S. V.; Eloul, S.; Katelhon, E.; Batchelor-McAuley, C.; Compton, R. G., Electrode-Particle Impacts: A Users Guide. *Phys. Chem. Chem. Phys.* **2017**, *19*, 28-43.
23. Stevenson, K. J.; Tschulik, K., A Materials Driven Approach for Understanding Single Entity Nano Impact Electrochemistry. *Current Opinion in Electrochemistry* **2017**, *6*, 38-45.
24. Allerston, L. K.; Rees, N. V., Nanoparticle Impacts in Innovative Electrochemistry. *Current Opinion in Electrochemistry* **2018**, *10*, 31-36.
25. Zhou, Y. G.; Rees, N. V.; Compton, R. G., The Electrochemical Detection and Characterization of Silver Nanoparticles in Aqueous Solution. *Angew. Chem. Int. Ed.* **2011**, *50*, 4219-4221.

26. Saw, E. N.; Kratz, M.; Tschulik, K., Time-Resolved Impact Electrochemistry for Quantitative Measurement of Single-Nanoparticle Reaction Kinetics. *Nano Research* **2017**, *10*, 3680-3689.
27. Lees, J. C.; Ellison, J.; Batchelor-McAuley, C.; Tschulik, K.; Damm, C.; Omanović, D.; Compton, R. G., Nanoparticle Impacts Show High-Ionic-Strength Citrate Avoids Aggregation of Silver Nanoparticles. *ChemPhysChem* **2013**, *14*, 3895-3897.
28. Wan, Y.; Guo, Z.; Jiang, X.; Fang, K.; Lu, X.; Zhang, Y.; Gu, N., Quasi-Spherical Silver Nanoparticles: Aqueous Synthesis and Size Control by the Seed-Mediated Lee–Meisel Method. *J. Colloid Interface Sci.* **2013**, *394*, 263-268.
29. Li, X.; Batchelor-McAuley, C.; Novev, J. K.; Compton, R. G., A Thermostated Cell for Electrochemistry: Minimising Natural Convection and Investigating the Role of Evaporation and Radiation. *Phys. Chem. Chem. Phys.* **2018**, *20*, 11794-11804.
30. Batchelor-McAuley, C.; Ellison, J.; Tschulik, K.; Hurst, P. L.; Boldt, R.; Compton, R. G., In Situ Nanoparticle Sizing with Zeptomole Sensitivity. *Analyst* **2015**, *140*, 5048-5054.
31. Kätelhön, E.; Feng, A.; Cheng, W.; Eloul, S.; Batchelor-McAuley, C.; Compton, R. G., Understanding Nano-Impact Current Spikes: Electrochemical Doping of Impacting Nanoparticles. *J. Phys. Chem. C* **2016**, *120*, 17029-17034.
32. Sun, P.; Mirkin, M. V., Kinetics of Electron-Transfer Reactions at Nanoelectrodes. *Anal. Chem.* **2006**, *78*, 6526-6534.
33. Little, C. A.; Xie, R.; Batchelor-Mcauley, C.; Kätelhön, E.; Li, X.; Young, N. P.; Compton, R. G., A Quantitative Methodology for the Study of Particle-Electrode Impacts. *Phys. Chem. Chem. Phys.* **2018**, *20*, 13537-13546.
34. Ellison, J.; Tschulik, K.; Stuart, E. J. E.; Jurkschat, K.; Omanović, D.; Uhlemann, M.; Crossley, A.; Compton, R. G., Get More out of Your Data: A New Approach to Agglomeration and Aggregation Studies Using Nanoparticle Impact Experiments. *ChemistryOpen* **2013**, *2*, 69-75.
35. de Mello Donegá, C., *Nanoparticles: Workhorses of Nanoscience*; Springer Berlin Heidelberg, 2014.
36. Sokolov, S. V.; Kätelhön, E.; Compton, R. G., Near-Wall Hindered Diffusion in Convective Systems: Transport Limitations in Colloidal and Nanoparticulate Systems. *J. Phys. Chem. C* **2016**, *120*, 10629-10640.
37. Ngamchuea, K.; Clark, R. O. D.; Sokolov, S. V.; Young, N. P.; Batchelor-McAuley, C.; Compton, R. G., Single Oxidative Collision Events of Silver Nanoparticles: Understanding the Rate-Determining Chemistry. *Chem. Eur. J.* **2017**, *23*, 16085-16096.
38. Krause, K. J.; Brings, F.; Schnitker, J.; Kätelhön, E.; Rinklin, P.; Mayer, D.; Compton, R. G.; Lemay, S. G.; Offenhäusser, A.; Wolfrum, B., The Influence of Supporting Ions on the Electrochemical Detection of Individual Silver Nanoparticles: Understanding the Shape and Frequency of Current Transients in Nano-Impacts. *Chem. Eur. J.* **2017**, *23*, 4638-4643.
39. Derjaguin, B.; Landau, L., Theory of the Stability of Strongly Charged Lyophobic Sols and of the Adhesion of Strongly Charged-Particles in Solutions of Electrolytes. *Prog Surf Sci* **1993**, *43*, 30-59.
40. Verwey, E. J. W., Theory of the Stability of Lyophobic Colloids. *J Phys Colloid Chem* **1947**, *51*, 631-636.
41. Kätelhön, E.; Cheng, W.; Batchelor-Mcauley, C.; Tschulik, K.; Compton, R. G., Nanoparticle-Impact Experiments Are Highly Sensitive to the Presence of Adsorbed Species on Electrode Surfaces. *ChemElectroChem* **2014**, *1*, 1057-1062.
42. Sokolov, S. V.; Tschulik, K.; Batchelor-McAuley, C.; Jurkschat, K.; Compton, R. G., Reversible or Not? Distinguishing Agglomeration and Aggregation at the Nanoscale. *Anal. Chem.* **2015**, *87*, 10033-10039.
43. Kätelhön, E.; Sokolov, S. V.; Bartlett, T. R.; Compton, R. G., The Role of Entropy in Nanoparticle Agglomeration. *ChemPhysChem* **2017**, *18*, 51-54.
44. Ung, T.; Giersig, M.; Dunstan, D.; Mulvaney, P., Spectroelectrochemistry of Colloidal Silver. *Langmuir* **1997**, *13*, 1773-1782.

45. Kelly, K. L.; Coronado, E.; Zhao, L. L.; Schatz, G. C., The Optical Properties of Metal Nanoparticles: The Influence of Size, Shape, and Dielectric Environment. *J. Phys. Chem. B* **2003**, *107*, 668-677.
46. Bhui, D. K.; Bar, H.; Sarkar, P.; Sahoo, G. P.; De, S. P.; Misra, A., Synthesis and Uv–Vis Spectroscopic Study of Silver Nanoparticles in Aqueous S D S Solution. *Journal of Molecular Liquids* **2009**, *145*, 33-37.

For TOC only